Johann Radon Institute for
Computational and Applied Mathematics
Austrian Academy of Sciences (ÖAW)

Multilevel preconditioning of elliptic problems discretized by a class of discontinuous Galerkin methods

J. Kraus, S. Tomar

RICAM-Report 2006-36

MULTILEVEL PRECONDITIONING OF ELLIPTIC PROBLEMS DISCRETIZED BY A CLASS OF DISCONTINUOUS GALERKIN METHODS

J. K. KRAUS† AND S. K. TOMAR†

Abstract. We present optimal order preconditioners for certain discontinuous Galerkin (DG) finite element discretizations of elliptic boundary value problems. A specific assembling process is proposed which allows us to use the hierarchy of geometrically nested meshes. We consider two variants of hierarchical splittings and study the angle between the resulting subspaces. Applying the corresponding two-level basis transformation recursively a sequence of algebraic problems is generated that can be associated with a hierarchy of coarse versions of DG approximations of the original problem. New bounds for the constant γ in the strengthened Cauchy-Bunyakowski-Schwarz inequality are derived. The presented numerical results support the theoretical analysis and demonstrate the potential of this approach.

Key words. Discontinuous Galerkin FEM, multilevel preconditioning, hierarchical basis, CBS constant

AMS subject classifications. 65N30, 65N22, 65N55

1. Introduction. Discontinuous Galerkin (DG) finite element (FE) methods for elliptic and parabolic problems have already been there for quite some time in the framework of interior penalty methods, see [1, 16, 29]. However, during the last decade they have seen much interest, particularly due to their suitability for *hp*-adaptive techniques, and are being applied to a variety of problems in various fields, see [28], the review article [14] and the references therein. They offer several advantages, e.g. the ease of treatment of meshes with hanging nodes, elements of varying shape and size, polynomials of variable degree, parallelization, preservation of local conservation properties, etc. An excellent overview and a detailed analysis of DG methods for elliptic problems can be found in [2, 13]. However, these methods come with an excessive number of degrees of freedom (DOF) as compared to their counter-part, i.e. the standard FE methods. It thus necessitates the development of efficient preconditioning techniques yielding fast iterative solvers.

Optimal-order preconditioners obtained from recursive application of two-level FE methods have been introduced and extensively analyzed in the context of conforming methods, see e.g., [3, 4, 5, 6, 9]. More recently, some extensions related to Crouzeix-Raviart or Rannacher-Turek nonconforming finite elements have also been considered [11, 18]. In this paper we address a different class of nonconforming methods which arises from certain DG-FE discretizations. We consider here the interior penalty (IP) DG method, however, our approach is applicable to other formulations with a similar stabilization term.

Geometric multigrid (MG) type preconditioners and solvers for the linear system of equations arising from DG discretizations have been considered in [12, 19, 20]. However, we approach this topic within the framework of algebraic multilevel techniques. In this context, recently, a projection technique has been proposed which is based on the idea of first smoothing and then projecting onto a coarse (auxiliary) space [15, 23]. The auxiliary space is related to a standard Galerkin discretization using

†Johann Radon Institute for Computational and Applied Mathematics, Austrian Academy of Sciences, Altenbergerstrasse 69, A-4040 Linz, Austria. ({johannes.kraus,satyendra.tomar}@oeaw.ac.at)

(a) continuous piece-wise linear functions, (b) Crouzeix-Raviart nonconforming FE functions, or (c) discontinuous piece-wise constant functions on the original partition of the domain. The latter choice, associated with the so-called "graph-Laplacian", has been further studied in [22].

In our approach we avoid this decomposition. Instead, we generate a sequence of algebraic problems that can be associated with a hierarchy of coarse versions of DG approximations of the original problem. Using geometrically nested meshes, together with a specific splitting of the terms in the bilinear form, we create a sequence of nested FE spaces and conduct the analysis of the proposed multilevel preconditioner. This splitting allows the assembling process to be similar to that of the conforming methods.

We consider a local definition of different variants of hierarchical splittings. We then derive new bounds for the constant γ in the strengthened Cauchy-Bunyakowski-Schwarz inequality which measures the quality of the underlying splitting. In the limiting case of the penalty parameter of the IP-DG method approaching infinity, the bounds correspond to those for the conforming (bilinear) elements.

We now briefly summarize the contents of the paper. We present the DG approximation of the second order elliptic problem in Section 2, which covers tessellation, function spaces, trace operators and the bilinear form. Discrete formulation and matrix assembly are parts of Section 3, where we present a specific splitting of the terms in the bilinear form resulting in an alternative assembling process. Two- and multi-level preconditioning with algebraic stabilization of the condition number is briefly recalled in Section 4. In Section 5 we discuss the two-level hierarchical basis transformation and propose two transformation variants for the IP-DG discretization. The analysis of the associated angle between the induced subspaces is the subject of the next section. Finally, numerical experiments are presented in Section 7 and conclusions are drawn in Section 8.

2. DG approximation of the second order elliptic problem. Consider a second order elliptic problem on a bounded Lipschitz domain $\Omega \subset \mathbb{R}^2$:

$$-\nabla \cdot (\underline{A}(x)\nabla u) = \underline{f}(x) \qquad \text{in } \Omega, \tag{2.1a}$$

$$u(x) = u_D \qquad \text{on } \Gamma_D, \tag{2.1b}$$

$$\underline{A}\nabla u \cdot \mathbf{n} = u_N \qquad \text{on } \Gamma_N. \tag{2.1c}$$

Here $\mathbf{n}$ is the exterior unit normal vector to $\partial\Omega \equiv \Gamma$. The boundary is assumed to be decomposed into two disjoint parts Γ_D and Γ_N, and the boundary data u_D, u_N are smooth. For the DG formulation below we shall need the existence of the traces of u and $\underline{A}\nabla u \cdot \mathbf{n}$ on the interfaces in Ω, and the solution u is assumed to have the required regularity. For the sake of simplicity, we assume that u_D is such that the boundary condition can be exactly satisfied by the approximations used. It is assumed that $\underline{A}$ is a symmetric positive definite matrix such that

$$c_1 |\xi|^2 \leqslant \underline{A}\xi \cdot \xi \leqslant c_2 |\xi|^2 \qquad \forall \xi \in \mathbb{R}^2.$$

Let $\mathcal{T}_h$ be a tessellation of Ω into a finite number of elements e with boundaries ∂e. Let N_e be the total number of elements in the mesh. For each finite element we denote its size by h_e and the mesh size of the partition by $h = \max_{e\in\mathcal{T}_h} h_e$. Now, as shown in Figure 2.1, let $f = \bar{e}^+ \cap \bar{e}^-$ be the interface of two adjacent elements e^+ and e^-. The set of all such internal interfaces is denoted by $\mathcal{F}_0$. Further, $\mathcal{F}_D$ and $\mathcal{F}_N$ will be the set of faces of elements on the boundary Γ_D and Γ_N, respectively.

Finally, $\mathcal{F}$ will be the set of all faces: $\mathcal{F} = \mathcal{F}_0 \cup \mathcal{F}_D \cup \mathcal{F}_N$. We denote the union of the faces of the elements e of $\mathcal{T}_h$ by Γ, i.e. $\Gamma = \cup_{e=1}^{N_e} \partial e$ and the union of the internal faces by Γ_0, i.e. $\Gamma_0 = \Gamma \backslash \partial\Omega$. We assume that the partition is shape-regular, see [26]. Though in this article we restrict ourselves to the case of uniform meshes, the approach discussed here can in principle be extended to finite elements of varying size and/or shape and nonconforming meshes (i.e., possessing hanging nodes). We also assume that the partition $\mathcal{T}_h$ is of bounded variation, i.e. there exists a constant $C_{\mathcal{T}_h}$ independent of the mesh size h such that for any two adjacent elements e and e' sharing a non-trivial part of a common interior face the following relation holds

$$\frac{h_e}{h_{e'}} \leqslant C_{\mathcal{T}_h}.$$

Further, the face measure h_f is constant on each face $f \in \mathcal{F}$ such that

$$h_f \coloneqq h_f(x) = |f|, \text{for} \quad x \in f \in \mathcal{F}.$$

On the partition $\mathcal{T}_h$ we define the "broken Sobolev space":

$$\mathcal{V} \coloneqq H^2(\mathcal{T}_h) = \{v \in L^2(\Omega) : \quad v|_e \in H^2(e), \quad \forall e \in \mathcal{T}_h\}.$$

Note that the functions in $\mathcal{V}$ **may not satisfy** any boundary conditions. We also define the finite dimensional space

$$\mathcal{V}_h \coloneqq \mathcal{V}_h(\mathcal{T}_h) = \{v \in L^2(\Omega) : v|_e \in P_r(e), \ \forall e \in \mathcal{T}_h\},$$

where P_r is the set of polynomials of degree $r \geqslant 1$. Obviously, $\mathcal{V}_h = \Pi_{e \in \mathcal{T}_h} P_r(e)$. For ease of the notations in what follows, we define on $\mathcal{V}$

$$(\underline{A}\nabla_h u_h, \nabla_h v_h)_{\mathcal{T}_h} \coloneqq \sum_{e \in \mathcal{T}_h} \int_e \underline{A}\nabla_h u_h \cdot \nabla_h v_h dx, \quad \langle p, q \rangle_{\mathcal{F}^g} \coloneqq \sum_{f \in \mathcal{F}^g} \int_f p \cdot q ds,$$

where $\mathcal{F}^g$ is one of the sets $\mathcal{F}$, $\mathcal{F}_0$, $\mathcal{F}_D$, $\mathcal{F}_N$ or their combinations.

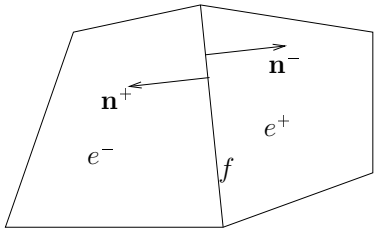

FIG. 2.1. *Two adjacent finite elements sharing a common interface f*

To deal with multivalued traces at the element boundary faces in a DG discretization we introduce some trace operators. This helps us to manipulate the numerical fluxes and to define the primal DG formulation. For $v \in \mathcal{V}$ we define the *average* ($\{.\}$) and *jump* ($[\![.]\!]$) as follows:
Let f be an interior face shared by elements e^+ and e^-. Define the unit normal vectors $\mathbf{n}^+$ and $\mathbf{n}^-$ on f pointing exterior to e^+ and e^-, respectively. With $v^{+/-} \coloneqq v|_{\partial e^{+/-}}$ we set

$$\{v\} = \frac{1}{2}\left(v^+ + v^-\right), \qquad [\![v]\!] = v^+\mathbf{n}^+ + v^-\mathbf{n}^- \quad \text{on } f \in \mathcal{F}_0.$$

For a piece-wise smooth vector function $\mathbf{q} \in [\mathcal{V}]^2$ we define $\mathbf{q}^{+/-}$ analogously, and set

$$\{\mathbf{q}\} = \frac{1}{2}\left(\mathbf{q}^+ + \mathbf{q}^-\right), \qquad [\![\mathbf{q}]\!] = \mathbf{q}^+ \cdot \mathbf{n}^+ + \mathbf{q}^- \cdot \mathbf{n}^- \quad \text{on } f \in \mathcal{F}_0.$$

Note, on E the jump of a scalar function is a vector, while the jump of a vector function is a scalar. For $f \in \mathcal{F}_D \cup \mathcal{F}_N$ each v and $\mathbf{q}$ have a uniquely defined restriction and we set

$$[\![v]\!] = v\mathbf{n}, \qquad \{\mathbf{q}\} = \mathbf{q}.$$

Since we do not require either of the quantities $\{v\}$ or $[\![\mathbf{q}]\!]$ on boundary faces we leave them undefined.

Finally, we shall use the following norm on $\mathcal{V}$:

$$\|v_h\|_*^2 = (\underline{A}\nabla_h v_h, \nabla_h v_h)_{\mathcal{T}_h} + \alpha h_f^{-1} \langle [\![v_h]\!], [\![v_h]\!] \rangle_{\mathcal{F}_0 \cup \mathcal{F}_D}. \tag{2.2}$$

Using the IP-DG formulation proposed by Arnold [1, 2] the primal DG formulation for the problem 2.1 can now be stated as follows:
Find $u_h \in \mathcal{V}$ such that for all $v_h \in \mathcal{V}$ the following relation holds:

$$\mathcal{A}(u_h, v_h) = \mathcal{L}(v_h), \tag{2.3a}$$

where the bilinear form $\mathcal{A}(u_h, v_h) : \mathcal{V} \times \mathcal{V} \to \mathbb{R}$ and the linear form $\mathcal{L}(v_h) : \mathcal{V} \to \mathbb{R}$ are defined as

$$\begin{aligned}
\mathcal{A}(u_h, v_h) =& (\underline{A}\nabla_h u_h, \nabla_h v_h)_{\mathcal{T}_h} + \alpha h_f^{-1} \langle [\![u_h]\!], [\![v_h]\!] \rangle_{\mathcal{F}_0 \cup \mathcal{F}_D} \\
&- \langle \{\underline{A}\nabla_h u_h\}, [\![v_h]\!] \rangle_{\mathcal{F}_0 \cup \mathcal{F}_D} - \langle [\![u_h]\!], \{\underline{A}\nabla_h v_h\} \rangle_{\mathcal{F}_0 \cup \mathcal{F}_D}, \qquad (2.3b) \\
\mathcal{L}(v_h) =& \int_\Omega \underline{f} v_h dx + \alpha h_f^{-1} \langle u_D, v_h \rangle_{\mathcal{F}_D} - \langle u_D \mathbf{n}, \underline{A}\nabla_h v_h \rangle_{\mathcal{F}_D} + \langle u_N, v_h \rangle_{\mathcal{F}_N}, \qquad (2.3c)
\end{aligned}$$

with α a sufficiently large stabilization parameter. For an explicit expression for α see [27]. The bilinear form $\mathcal{A}$ is coercive and bounded in $\mathcal{V}$ equipped with the norm (2.2) for $\alpha > 0$ sufficiently large, see [2]. Further, for $f \in L^2(\Omega)$ we have a unique solution $u_h \in \mathcal{V}$.

3. Discrete formulation and matrix assembly. The weak formulation (2.3) is transformed into a set of algebraic equations by approximating u_h and v_h using linear polynomials in each element as

$$u_{e,h} = \sum_{j=0}^{3} \widetilde{u}_{e,j} \mathcal{N}_{e,j}(x), \quad v_{e,h} = \sum_{j=0}^{3} \widetilde{v}_{e,j} \mathcal{N}_{e,j}(x), \quad x \in e \subset \mathbb{R}^2. \tag{3.1}$$

Here $\widetilde{u}_{e,j} \in \mathbb{R}^4$ and $\widetilde{v}_{e,j} \in \mathbb{R}^4$ are the expansion coefficients of u_h and the test function v_h in the element e, respectively, and $\mathcal{N}_{e,j}$ are the bilinear basis functions.

We now briefly show the computation of the element stiffness matrix. Consider a general element e with all its face internal. Let its neighboring elements, which share a face with this element, be denoted by e_1^+, e_2^+, e_3^+, and e_4^+. Here $\cdot^+$ represents the neighboring element and digits $1, \ldots, 4$ represent the face number with which the neighboring element is attached. This arrangement is depicted in Figure 3.1.

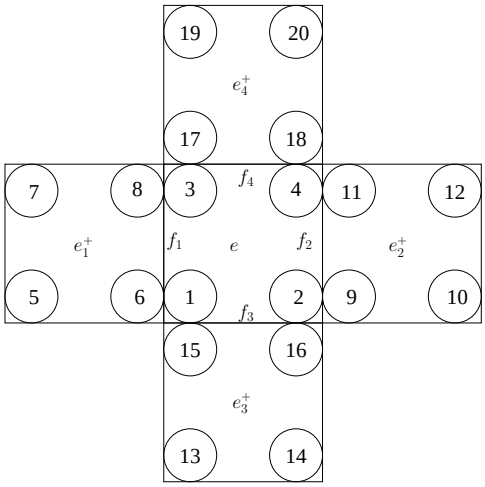

FIG. 3.1. *Standard arrangement of elemental DOF*

The bilinear form for this element reads:

$$\bar{\mathcal{A}}_e(u_h, v_h) = \int_e \underline{A}\nabla_h u_h \cdot \nabla_h v_h dx + \alpha h_f^{-1} \sum_{f\in\partial e} \int_f [\![u_h]\!] \cdot [\![v_h]\!]\, ds$$
$$- \sum_{f\in\partial e} \int_f \left(\{\underline{A}\nabla_h u_h\} \cdot [\![v_h]\!] + [\![u_h]\!] \cdot \{\underline{A}\nabla_h v_h\}\right) ds. \tag{3.2}$$

Using the definition of trace operators $\{\cdot\}$ and $[\![\cdot]\!]$ and, as a standard procedure, collecting the terms with the test function for the element e we get

$$\mathring{\mathcal{A}}_e(u_h, v_h) = \int_e \underline{A}\nabla_h u_h \cdot \nabla_h v_h dx + \alpha h_f^{-1} \sum_{s=1}^{4} \int_{f_s} v_e \mathbf{n}_e \cdot \left(u_e \mathbf{n}_e + u_{e_s^+} \mathbf{n}_{e_s^+}\right) ds$$
$$- \frac{1}{2} \sum_{s=1}^{4} \int_{f_s} \left(v_e \mathbf{n}_e \cdot \left(\underline{A}\nabla_h u_e + \underline{A}\nabla_h u_{e_s^+}\right)\right.$$
$$\left. + \underline{A}\nabla_h v_e \cdot \left(u_e \mathbf{n}_e + u_{e_s^+} \mathbf{n}_{e_s^+}\right)\right) ds. \tag{3.3}$$

Before proceeding further we now introduce the following matrices in $\mathbb{R}^{4\times 4}$: C_e, $B_{ee^+;s}$, and $E_{ee^+;s}$, with the components

$$C_{e;ij} = \int_e \underline{A}\nabla_h \mathcal{N}_{e,i} \cdot \nabla_h \mathcal{N}_{e,j} dx, \tag{3.4a}$$
$$B_{ee^+;s;ij} = \int_{f_s} \mathcal{N}_{e,i} n_e \cdot \underline{A}\nabla_h \mathcal{N}_{e^+,j} ds, \tag{3.4b}$$
$$E_{ee^+;s;ij} = \int_{f_s} \mathcal{N}_{e,i} \mathcal{N}_{e^+,j} ds. \tag{3.4c}$$

Substituting these matrices in (3.3) and using the fact that $\mathbf{n}_e \cdot \mathbf{n}_e = 1$ and $\mathbf{n}_e \cdot \mathbf{n}_{e^+} = -1$

we get the following element stiffness matrix for e

$$\begin{aligned}\mathring{A}_e =& C_e + \sum_{s=1}^{4} \Big(\alpha h_f^{-1}(E_{ee;s} - E_{ee^+;s}) \\ & - \frac{1}{2}(B_{ee;s} + B_{ee;s}^T + B_{ee^+;s} + B_{e^+e;s}^T)\Big),\end{aligned} \tag{3.5}$$

where $\cdot^T$ denotes the transpose of the matrix.

The size of the resulting matrix $\mathring{A}_e$ is 4×20 since, as depicted in Figure 3.1, the DOF of the element e are connected with all the DOF of its neighboring elements e_s^+. This will create severe difficulties in creating nested FE spaces with local support.

As an alternative, we propose the following simple approach. We note that the abovementioned difficulty is caused by the computation of the $\nabla_h u_{e^+}$ terms when associated with the element e. Hence, we split the terms in the elemental bilinear form (3.2) in such a way that the $\nabla_h u_{e^+}$ terms are used only in the computation of the respective element e^+, and thus, only the $\nabla_h u_e$ terms are associated with e. Moreover, in this arrangement, to avoid the singularity of the resulting stiffness matrix, we need to consider all parts of the stabilization term in (3.2). Since this would double the contribution from the respective terms in the global stiffness matrix we take them with the weight 1/2. The resulting elemental bilinear form is then given by

$$\begin{aligned}\mathcal{A}_e(u_h, v_h) = & \int_e \underline{A}\nabla_h u_h \cdot \nabla_h v_h dx - \frac{1}{2}\sum_{s=1}^{4}\int_{f_s} \Big(\Big(v_e\mathbf{n}_e + v_{e_s^+}\mathbf{n}_{e_s^+}\Big)\cdot \underline{A}\nabla_h u_e \\ & + \underline{A}\nabla_h v_e \cdot \Big(u_e\mathbf{n}_e + u_{e_s^+}\mathbf{n}_{e_s^+}\Big)\Big)\, ds \\ & + \frac{\alpha h_f^{-1}}{2}\sum_{s=1}^{4}\int_{f_s}\Big(v_e\mathbf{n}_e + v_{e_s^+}\mathbf{n}_{e_s^+}\Big)\cdot\Big(u_e\mathbf{n}_e + u_{e_s^+}\mathbf{n}_{e_s^+}\Big)\, ds.\end{aligned} \tag{3.6}$$

This gives us the following elemental stiffness matrix

$$\begin{aligned}A_e =& C_e + \sum_{s=1}^{4}\Big(\frac{\alpha h_f^{-1}}{2}(E_{ee;s} - E_{ee^+;s} - E_{e^+e;s} + E_{e^+e^+;s}) \\ & - \frac{1}{2}(B_{ee;s} + B_{ee;s}^T + B_{e^+e;s} + B_{e^+e;s}^T)\Big).\end{aligned} \tag{3.7}$$

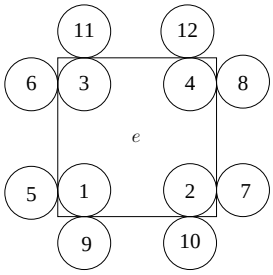

FIG. 3.2. *Specific arrangement of elemental DOF*

In this approach, as depicted in Figure 3.2, the DOF of the element e are connected with only those DOF of its neighboring elements e_s^+ which are at the common face. The size of the matrix A_e is 12×12 and the details are provided in the appendix A.

REMARK 3.1. *It is important to note that this specific splitting of terms in the bilinear form is possible only for some of the DG methods proposed in literature, e.g. which contains the α_j type stabilization term of [2]. These include the symmetric IP method [16], method of Baumann and Oden [10], its stabilized version NIPG [24], and the method of Babuška-Zlamal [8].*

REMARK 3.2. *This splitting is also advantageous when dealing with problems having jumps in the coefficient where jumps are aligned with element boundaries. This is due to the fact that the alternative approach requires $\underline{A}$ only from the current element, whereas in the standard approach one needs to take into account $\underline{A}$ from the neighboring elements also.*

Now let $N = 4N_e$ denote the total number of DOF in the system. Using the polynomial approximation (3.1) into the weak form (2.3), with elemental bilinear form (3.6), we get the following linear system of equations

$$A\mathbf{x} = \mathbf{b}, \tag{3.8}$$

where $\mathbf{x} \in \mathbb{R}^N$, $A \in \mathbb{R}^{N\times N}$ with N_e^2 blocks of size 4×4, and $\mathbf{b} \in \mathbb{R}^N$, denote the vector of expansion coefficients $\tilde{u}$, the global stiffness matrix, and the right hand side data vector, respectively.

4. Two- and multilevel preconditioning. In this Section we briefly recall the two- and multilevel preconditioning techniques with algebraic stabilization. For details we refer to [5, 6, 7, 21].

The multilevel methods, which are a recursive extension of two-level methods, lead to the class of hierarchical basis (HB) methods for which the condition number grows, in general, exponentially with the number of levels ℓ. We are interested in multilevel preconditioners $M^{(\ell)}$ which satisfy the property

$$\kappa({M^{(\ell)}}^{-1}A) = O(1),$$

independently of the discretization parameter h. This can be achieved by combining HB preconditioners with various types of stabilization techniques, such as algebraic multilevel iteration (AMLI) methods. The stabilization of the condition number can be achieved either by employing a specially constructed matrix polynomial P_{β_k} of degree β_k on some (or all) levels $k = k_0 + 1, \cdots, \ell$, or using some fixed small number of inner generalized conjugate gradient (GCG) iterations, the first approach corresponding to linear AMLI (LAMLI) and the latter to nonlinear AMLI (NLAMLI) [21].

Starting from the coarsest mesh (level 0) with $M^{(0)} = A^{(0)}$, the basic idea is to apply the following multiplicative two-level preconditioner recursively at all levels $k = 1, 2, \ldots, \ell$ of mesh refinement

$$M^{(k)} = \begin{bmatrix} C_{11}^{(k)} & 0 \\ \widehat{A}_{21}^{(k)} & C_{22}^{(k)} \end{bmatrix} \begin{bmatrix} I & {C_{11}^{(k)}}^{-1}\widehat{A}_{12}^{(k)} \\ 0 & I \end{bmatrix}, \tag{4.1}$$

where $C_{11}^{(k)}$ is a preconditioner for the upper-left pivot block of the (hierarchical) stiffness matrix

$$\widehat{A}^{(k)} = \begin{bmatrix} \widehat{A}_{11}^{(k)} & \widehat{A}_{12}^{(k)} \\ \widehat{A}_{21}^{(k)} & \widehat{A}_{22}^{(k)} \end{bmatrix},$$

and the matrix $C_{22}^{(k)}$ is implicitly given by the equation

$$C_{22}^{(k)^{-1}} = \left[I - P_\beta \left(M^{(k-1)^{-1}} \widehat{A}^{(k-1)} \right) \right] \widehat{A}^{(k-1)^{-1}}. \tag{4.2}$$

Here $M^{(k-1)}$ and $\widehat{A}^{(k-1)}$ denote the multiplicative preconditioner and the stiffness matrix, respectively, at level $(k-1)$, and $\widehat{A}^{(0)} = A^{(0)}$ by definition. Then, as well known from theory [5, 6], a properly shifted Chebyshev polynomial P_β of degree $\beta \in \{2, 3\}$, satisfying the conditions

$$0 \leqslant P_\beta(t) < 1, \quad 0 < t \leqslant 1, \quad P_\beta(0) = 1,$$

can be used to stabilize the condition number of the LAMLI preconditioner. The whole iterative solution process is of optimal computational complexity if the degree $\beta_k = \beta$ of the matrix polynomial (or alternatively, the number of inner iterations at level k for NLAMLI) satisfies the condition

$$1/\sqrt{(1-\gamma^2)} < \beta < \tau, \tag{4.3}$$

where $\tau \approx N_k/N_{k-1}$ denotes the reduction factor of the number of DOF, and γ denotes the constant in the strengthened Cauchy-Bunyakowski-Schwarz (CBS) inequality, cf. Section 6. The exact value of τ for DG approximations of 2D problems is 4.

5. Two-level hierarchical basis transformation. Hierarchical bases (HB), in the present context, are related to a sequence of hierarchical meshes, which may or may not produce a nested sequence of finite element spaces. For that reason we consider a hierarchy of partitions $\mathcal{T}_{h_\ell} \subset \mathcal{T}_{h_{\ell-1}} \subset \ldots \subset \mathcal{T}_{h_1} \subset \mathcal{T}_{h_0}$ of Ω, where the notation $\mathcal{T}_{h_k} = \mathcal{T}_h \subset \mathcal{T}_H = \mathcal{T}_{h_{k-1}}$ means that for any element e of the fine(r) partition $\mathcal{T}_h$ there is an element E of the coarse(r) mesh partition $\mathcal{T}_H$ such that $e \subset E$.

In this section we will introduce the hierarchical basis transformation generating two levels of a discrete DG system; the multilevel extension is obtained by a recursive application of the two-level transformation to the coarse-level system.

Consider the linear system (3.8) resulting from the IP-DG approximation of the basic problem (2.1). The partitioning of variables (and corresponding equations) into a *fine* and a *coarse* (sub-) set, indicated by the subscripts 1 and 2, respectively, is caused by a regular mesh refinement at every level $(k-1) = 0, 1, \ldots, \ell-1$. This means that by halving the meshsize, i.e., $h = H/2$, each element is subdivided into four elements of similar shape, herewith producing the mesh at levels $k = 1, 2, \ldots, \ell$. Hence, the linear system (3.8) can be represented in the 2×2 block form as

$$\begin{bmatrix} A_{11} & A_{12} \\ A_{21} & A_{22} \end{bmatrix} \begin{pmatrix} \mathbf{x}_1 \\ \mathbf{x}_2 \end{pmatrix} = \begin{pmatrix} \mathbf{b}_1 \\ \mathbf{b}_2 \end{pmatrix} \tag{5.1}$$

where $A_{21} = A_{12}^T$. Now, if we make use of the two-level transformation matrix

$$J = \begin{bmatrix} I_{11} & P_{12} \\ 0 & I_{22} \end{bmatrix}, \tag{5.2}$$

the system to be solved in the hierarchical basis reads

$$\widehat{A}\,\widehat{\mathbf{x}} = \widehat{\mathbf{b}}. \tag{5.3}$$

The matrix $\widehat{A}$ and its submatrices $\widehat{A}_{11}$, $\widehat{A}_{12}$ $\widehat{A}_{21}$, $\widehat{A}_{22}$ are given by

$$\widehat{A} = J^T A\, J = \begin{bmatrix} \widehat{A}_{11} & \widehat{A}_{12} \\ \widehat{A}_{21} & \widehat{A}_{22} \end{bmatrix},$$

$$\widehat{A}_{11} = A_{11}, \quad \widehat{A}_{12} = A_{11}P_{12} + A_{12}, \quad \widehat{A}_{21} = P_{12}^T A_{11} + A_{21}, \tag{5.4a}$$

$$\widehat{A}_{22} = P_{12}^T A_{11} P_{12} + A_{21}P_{12} + P_{12}^T A_{12} + A_{22} \tag{5.4b}$$

The vectors $\widehat{\mathbf{x}}$ and $\widehat{\mathbf{b}}$ are transformed then from hierarchical basis to a nodal basis via $\mathbf{x} = J\,\widehat{\mathbf{x}}$ and $\widehat{\mathbf{b}} = J^T\mathbf{b}$, and the following relations hold

$$\mathbf{x}_1 = \widehat{\mathbf{x}}_1 + P_{12}\widehat{\mathbf{x}}_2, \quad \mathbf{x}_2 = \widehat{\mathbf{x}}_2, \tag{5.5a}$$

$$\widehat{\mathbf{b}}_1 = \mathbf{b}_1, \qquad \widehat{\mathbf{b}}_2 = P_{12}^T\mathbf{b}_1 + \mathbf{b}_2. \tag{5.5b}$$

REMARK 5.1. *The choice $P_{12} = -A_{11}^{-1}A_{12}$ yields the block-diagonal matrix*

$$\widehat{A} = \begin{bmatrix} A_{11} & 0 \\ 0 & S \end{bmatrix}$$

with $S = A_{22} - A_{21}A_{11}^{-1}A_{12}$ being the exact Schur complement arising from elimination of the fine DOF. Although this results in an orthogonal decomposition of the finite element space into a coarse space and its complement, i.e., the best possible CBS constant $\gamma = 0$, one will not be able to compute this representation at reasonable costs in practice because the inversion of A_{11} is too expensive and the exact Schur complement typically is a dense matrix.

When constructing the global interpolation P_{12} we aim at achieving that

(a) P_{12} (and thus J) becomes a sparse matrix with $\mathcal{O}(1)$ entries in each row.
(b) $\widehat{A}_{22} = P_{12}^T A_{11} P_{12} + A_{21}P_{12} + P_{12}^T A_{12} + A_{22}$ has a structure and sparsity pattern similar to that of A and defines an adequate coarse-grid problem. In particular, when dealing with the pure Neumann problem, this implies the necessary condition $\ker(\widehat{A}_{22}) = \ker(S)$.
(c) P_{12} can be defined locally for a set of macro elements $\{E\}$ that covers the whole mesh, i.e., given a macro element interpolation matrix P_E for all $E \in \mathcal{T}_H$ the matrix P_{12} is uniquely defined.

In practice, the property (a) guarantees that matrix-vector products involved in the hierarchical basis representation, which, based on the identities (5.4a)–(5.5b), do not require an explicit evaluation of the HB matrices (5.4a)–(5.4b), can be performed with computational costs proportional to the number of fine or coarse DOF. The property (b) is important for constructing an efficient two-level method and also for applying the two-level procedure recursively in order to obtain a full multilevel method. Finally, the property (c) is desirable for controlling the sparsity pattern of the two-level transformation, and consequently, controlling the stencil of the coarse-grid operator. It further provides an opportunity for a local analysis of the derived two- and multilevel preconditioners.

The general macro element we are using to define the local interpolation P_E is depicted in Figure 5.1. It is important to note that the nonzero pattern and the entries of P_E have to be defined in such a way that the local interpolation (for neighboring macro elements) is compatible, i.e., the stencil and the coefficients have to agree for

fine nodes shared by adjacent macro elements (in 2D these are at most 2) in their respective local interpolation matrices P_E.

The local macro-element two-level transformation matrix J_E is given by

$$J_E = \begin{bmatrix} I & P_E \\ 0 & I \end{bmatrix}, \tag{5.6}$$

where the macro-element interpolation matrix P_E is of size 20×12. For symmetry reasons we consider transformations that can be characterized by the matrix P_E given below:

$$P_E = \begin{bmatrix}
p_1 & p_2 & p_2 & p_3 & p_4 & p_5 & p_5 & p_6 & p_4 & p_5 & p_5 & p_6 \\
p_2 & p_1 & p_3 & p_2 & p_5 & p_6 & p_4 & p_5 & p_5 & p_4 & p_6 & p_5 \\
p_2 & p_3 & p_1 & p_2 & p_5 & p_4 & p_6 & p_5 & p_5 & p_6 & p_4 & p_5 \\
p_3 & p_2 & p_2 & p_1 & p_6 & p_5 & p_5 & p_4 & p_6 & p_5 & p_5 & p_4 \\
q_1 & 0 & q_2 & 0 & q_3 & q_4 & 0 & 0 & 0 & 0 & 0 & 0 \\
q_2 & 0 & q_1 & 0 & q_4 & q_3 & 0 & 0 & 0 & 0 & 0 & 0 \\
0 & q_1 & 0 & q_2 & 0 & 0 & q_3 & q_4 & 0 & 0 & 0 & 0 \\
0 & q_2 & 0 & q_1 & 0 & 0 & q_4 & q_3 & 0 & 0 & 0 & 0 \\
q_1 & q_2 & 0 & 0 & 0 & 0 & 0 & 0 & q_3 & q_4 & 0 & 0 \\
q_2 & q_1 & 0 & 0 & 0 & 0 & 0 & 0 & q_4 & q_3 & 0 & 0 \\
0 & 0 & q_1 & q_2 & 0 & 0 & 0 & 0 & 0 & 0 & q_3 & q_4 \\
0 & 0 & q_2 & q_1 & 0 & 0 & 0 & 0 & 0 & 0 & q_4 & q_3 \\
q_3 & 0 & q_4 & 0 & q_1 & q_2 & 0 & 0 & 0 & 0 & 0 & 0 \\
q_4 & 0 & q_3 & 0 & q_2 & q_1 & 0 & 0 & 0 & 0 & 0 & 0 \\
0 & q_3 & 0 & q_4 & 0 & 0 & q_1 & q_2 & 0 & 0 & 0 & 0 \\
0 & q_4 & 0 & q_3 & 0 & 0 & q_2 & q_1 & 0 & 0 & 0 & 0 \\
q_3 & q_4 & 0 & 0 & 0 & 0 & 0 & 0 & q_1 & q_2 & 0 & 0 \\
q_4 & q_3 & 0 & 0 & 0 & 0 & 0 & 0 & q_2 & q_1 & 0 & 0 \\
0 & 0 & q_3 & q_4 & 0 & 0 & 0 & 0 & 0 & 0 & q_1 & q_2 \\
0 & 0 & q_4 & q_3 & 0 & 0 & 0 & 0 & 0 & 0 & q_2 & q_1
\end{bmatrix} \tag{5.7}$$

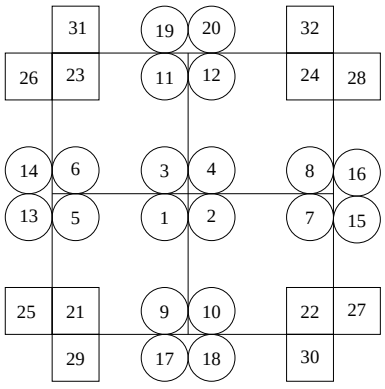

FIG. 5.1. *One macro element E*

For the problems under consideration, using similar arguments as presented in Section 6 one finds that choosing $p_4 = p_5 = p_6 = 0$ does not deteriorate the angle

associated with the splitting of the finite element space and since we are interested in keeping the transformation matrix as sparse as possible this motivates to study the following two particular choices of P_E which are based on simple averaging:

1. $J^{(1)}$ is induced by (5.6), P_E is given by (5.7), and $p_1 = p_2 = p_3 = 1/4$, $p_4 = p_5 = p_6 = 0$, $q_1 = q_2 = 1/2$, $q_3 = q_4 = 0$
2. $J^{(2)}$ is induced by (5.6), P_E is given by (5.7), and $p_1 = p_2 = p_3 = 1/4$, $p_4 = p_5 = p_6 = 0$, $q_1 = q_2 = q_3 = q_4 = 1/4$

Of course, the second scheme needs a modification at the boundaries such that the sum of interpolation coefficients always equals one.* We shall show that, however, the second variant performs better than the first one. The connections for a few internal and face DOF are depicted in Figure 5.2, where red and blue lines denote the weight 1/4 and 1/2, respectively. A similar treatment applies to other internal and face DOF.

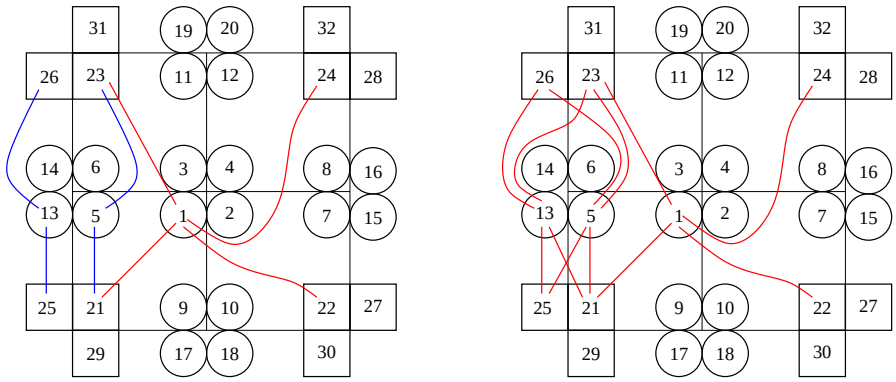

(a) Variant 1 (b) Variant 2

FIG. 5.2. *The connections of the DOF of a macro element*

6. Angle between the induced subspaces. It is known that the constant γ in the CBS inequality, which is associated with the abstract angle between the two subspaces induced by the two-level hierarchical basis transformation, plays a key role in the derivation of optimal convergence rate estimates for two- and multilevel methods. Moreover, the value of the upper bound for $\gamma \in (0, 1)$ is part of the construction of a proper stabilization polynomial in the linear algebraic multilevel iteration (LAMLI) method, see [5, 6].

For the constant γ in the strengthened CBS inequality, the following relation holds

$$\gamma = \cos(\mathcal{V}_1, \mathcal{V}_2) = \sup_{u \in \mathcal{V}_1,\ v \in \mathcal{V}_2} \frac{\mathcal{A}(u, v)}{\sqrt{\mathcal{A}(u, u)\mathcal{A}(v, v)}}, \tag{6.1}$$

where $\mathcal{A}(\cdot, \cdot)$ is the bilinear form given by (2.3b). If $\mathcal{V}_1 \cap \mathcal{V}_2 = \{0\}$ then γ is strictly less than one.

*For instance, a macro element touching the boundary with its left face – when DOF 13, 14, 25, 26 are missing – has the correct local interpolation coefficients 1/2 for each of the couplings between DOF 5 and 6 and the coarse DOF 21 and 23, which is the same as for the interpolation scheme 2, cf. Figure 5.1.

As shown in [4], the constant γ can be estimated locally over each macro-element $E \in \mathcal{T}_H$, i.e. $\gamma \leqslant \max_E \gamma_E$, where

$$\gamma_E = \sup_{u \in \mathcal{V}_1(E),\ v \in \mathcal{V}_2(E)} \frac{\mathcal{A}_E(u,v)}{\sqrt{\mathcal{A}_E(u,u)\mathcal{A}_E(v,v)}}, \quad v \neq \text{const.}$$

The abovementioned spaces $\mathcal{V}_m(E), m = 1, 2$, contain the functions from $\mathcal{V}_m$ restricted to E and $\mathcal{A}_E(u,v)$ corresponds to $\mathcal{A}(u,v)$ restricted to the macro element E (see also [17]).

Thus we have to consider the macro-element stiffness matrix $\widehat{A}_E$ obtained from assembling the element matrices for all elements e contained in E in the (local) hierarchical basis. Evidently, the global two-level stiffness matrix $\widehat{A}$ can be assembled from the macro-element two-level stiffness matrices, which we write using a simplified notation as

$$\widehat{A} = J^T A\, J = \sum_{E \in \mathcal{T}_H} \widehat{A}_E = \sum_{E \in \mathcal{T}_H} J_E^T A_E\, J_E.$$

Like the global matrix, the local matrices are also of the following 2×2 block form

$$\widehat{A}_E = \begin{bmatrix} \widehat{A}_{E,11} & \widehat{A}_{E,12} \\ \widehat{A}_{E,21} & \widehat{A}_{E,22} \end{bmatrix} = J_E^T \begin{bmatrix} A_{E,11} & A_{E,12} \\ A_{E,21} & A_{E,22} \end{bmatrix} J_E, \tag{6.2}$$

where J_E is defined by (5.6) and the local Schur complement is given by

$$S_E = \widehat{A}_{E,22} - \widehat{A}_{E,21}\widehat{A}_{E,11}^{-1}\widehat{A}_{E,12} = A_{E,22} - A_{E,21}A_{E,11}^{-1}A_{E,12}. \tag{6.3}$$

As we know from the general framework of two-level block (incomplete) factorization methods, it suffices to compute the minimal eigenvalue $\lambda_{E;\min}$ of the generalized eigenproblem

$$S_E \mathbf{v}_{E,2} = \lambda_E \widehat{A}_{E,22}\mathbf{v}_{E,2}, \quad \mathbf{v}_{E,2} \perp (1,1,\ldots,1)^T, \tag{6.4}$$

in order to conclude the following upper bound for the constant γ in (6.1):

$$\gamma^2 \leqslant \max_{E \in \mathcal{T}_H} \gamma_E^2 = \max_{E \in \mathcal{T}_H} (1 - \lambda_{E;\min}) \tag{6.5}$$

This relation then implies condition number estimates for the corresponding two-level preconditioner (of additive and multiplicative type), see, e.g., [3].

Let us therfore direct our attention to the solution of problem (6.4). Consider Variant 1 of the two-level basis transformation specified at the end of the last section. Using the macro-element matrix, which is obtained from assembling four equal element matrices $A_e(\alpha)$, see (A.1), the minimal eigenvalue $\lambda_{E;\min}^{(1)}$ of (6.4) is to be found

$$\lambda_{E;\min}^{(1)} = 1 - (\gamma_E^{(1)})^2 = \frac{1}{4}\left(1 - \frac{1}{2\alpha}\right). \tag{6.6}$$

This results in the bound

$$\gamma_E^{(1)} \leqslant \sqrt{\frac{3}{4} + \frac{1}{8\alpha}}\ . \tag{6.7}$$

In order to derive an estimate which holds true for all levels of mesh refinement and corresponding factorization steps, we need to repeat the calculation of γ_E, thereby replacing $A_e(\alpha)$ with $\widehat{A}_{E,22}$ when assembling the new macro-element matrix (at each subsequent level). In case of Variant 1 it turns out that the element matrices at successive levels fulfill the relation

$$\widehat{A}_{E,22} = A_e(2\alpha). \tag{6.8}$$

In other words, the coarse-grid matrix corresponds to the same kind of IP-DG discrete problem (on a mesh with spacing $H = 2 * h$) but using double the value for the stabilization parameter α. Even though this results in a smaller upper bound for $\gamma_E^{(1)}$, showing that inequality (6.7) is valid for all subsequent levels if it is valid for the first one, an additional difficulty arises, which is related to the preconditioning of the A_{11}-block.

The condition number of A_{11} is of order $\mathcal{O}(\alpha)$ and thus the block factorization in the hierarchical basis, when constructed using the transformation Variant 1, with increasing level number, in general, makes the solution of the sub-systems with A_{11} more and more difficult. Further, the bound (6.7) is slightly too weak in order to guarantee that the condition number of the multiplicative preconditioner (with exact inversion of the A_{11}-block) can be stabilized using Chebyshev polynomials of degree two. However, combining the optimality condition (4.3) with (6.7) we obtain $\alpha > 9/10$, which is to be satisfied for a condition number that can be uniformly bounded in the number of levels if one uses optimal third-order polynomial stabilization. Note that, however, the stability of the DG discretization scheme requires a larger α, see [27].

Let us next focus on Variant 2. As already exemplified, the local analysis of the multilevel algorithm involves the angle between the subspaces related to the two-level hierarchical basis transformation at every stage (of mesh refinement or coarsening). The following lemma provides the explicit form of the element matrix $A_e^{(j)}(\alpha)$ after j regular coarsening (unrefinement) steps, starting with the element matrix

$$A_e^{(0)}(\alpha) = A_e(\alpha) \tag{6.9}$$

at the fine-grid level ℓ, cf. equation (A.1).

LEMMA 6.1. *If we neglect boundary effects, the element matrix $A_e^{(j)}(\alpha)$ after j unrefinement steps, $1 \leqslant j < \ell$, is given by*

$$A_e^{(j)}(\alpha) = X_e(\alpha) + jY_e \tag{6.10}$$

where

$$X_e(\alpha) = \begin{bmatrix} X_{e,11}(\alpha) & X_{e,12}(\alpha) & X_{e,13}(\alpha) \\ X_{e,12}^T(\alpha) & X_{e,22}(\alpha) & X_{e,23}(\alpha) \\ X_{e,13}^T(\alpha) & X_{e,23}^T(\alpha) & X_{e,33}(\alpha) \end{bmatrix}, \; Y_e = \begin{bmatrix} Y_{e,11} & Y_{e,12} & Y_{e,13} \\ Y_{e,12}^T & Y_{e,22} & Y_{e,23} \\ Y_{e,13}^T & Y_{e,23}^T & Y_{e,33} \end{bmatrix},$$

$$X_{e,11}(\alpha) = \begin{bmatrix} \frac{\alpha}{3} & 0 & 0 & -\frac{1}{24} \\ 0 & \frac{\alpha}{3} & -\frac{1}{24} & 0 \\ 0 & -\frac{1}{24} & \frac{\alpha}{3} & 0 \\ -\frac{1}{24} & 0 & 0 & \frac{\alpha}{3} \end{bmatrix}, \; X_{e,22}(\alpha) = \begin{bmatrix} \frac{\alpha}{6} & \frac{1}{8} & 0 & 0 \\ \frac{1}{8} & \frac{\alpha}{6} & 0 & 0 \\ 0 & 0 & \frac{\alpha}{6} & \frac{1}{8} \\ 0 & 0 & \frac{1}{8} & \frac{\alpha}{6} \end{bmatrix},$$

$$X_{e,33}(\alpha) = X_{e,22}(\alpha),$$

$$X_{e,12}(\alpha) = \begin{bmatrix} \frac{1-\alpha}{6} & \frac{1}{48} & -\frac{5}{48} & -\frac{1}{16} \\ -\frac{5}{48} & -\frac{1}{16} & \frac{1-\alpha}{6} & \frac{1}{48} \\ \frac{1}{48} & \frac{1-\alpha}{6} & -\frac{1}{16} & -\frac{5}{48} \\ -\frac{1}{16} & -\frac{5}{48} & \frac{1}{48} & \frac{1-\alpha}{6} \end{bmatrix}, \; X_{e,13}(\alpha) = \begin{bmatrix} \frac{1-\alpha}{6} & \frac{1}{48} & -\frac{5}{48} & -\frac{1}{16} \\ \frac{1}{48} & \frac{1-\alpha}{6} & -\frac{1}{16} & -\frac{5}{48} \\ -\frac{5}{48} & -\frac{1}{16} & \frac{1-\alpha}{6} & \frac{1}{48} \\ -\frac{1}{16} & -\frac{5}{48} & \frac{1}{48} & \frac{1-\alpha}{6} \end{bmatrix},$$

$$X_{e,23}(\alpha) = X_{e,23} = \begin{bmatrix} 0 & -\frac{1}{16} & -\frac{1}{16} & -\frac{1}{48} \\ -\frac{1}{16} & -\frac{1}{48} & 0 & -\frac{1}{16} \\ -\frac{1}{16} & 0 & -\frac{1}{48} & -\frac{1}{16} \\ -\frac{1}{48} & -\frac{1}{16} & -\frac{1}{16} & 0 \end{bmatrix},$$

$$Y_{e,11} = \frac{1}{24}\, I, \quad Y_{e,22} = Y_{e,33} = \frac{1}{8}\, I, \quad Y_{e,13} = -\frac{1}{48}\, I,$$

$$Y_{e,12} = \begin{bmatrix} -\frac{1}{48} & 0 & 0 & 0 \\ 0 & 0 & -\frac{1}{48} & 0 \\ 0 & -\frac{1}{48} & 0 & 0 \\ 0 & 0 & 0 & -\frac{1}{48} \end{bmatrix}, \quad Y_{e,23} = 5\; Y_{e,12}.$$

Moreover, Y_e is SPSD with three fourfold eigenvalues, given by $11/48$, $1/16$, *and* 0*; and the matrix $X_e(\alpha)$ is SPSD iff $\alpha > 11/8$. Further, $X_e(\alpha)$ is monotonically increasing in α which means that $X_e(\alpha) - X_e(\alpha')$ is SPSD, i.e., $X_e(\alpha) - X_e(\alpha') \geqslant 0$ if $\alpha - \alpha' \geqslant 0$.*

Proof. The results can be verified by direct computations (using a Computer Algebra Program such as MATHEMATICA). □

In the local analysis of the multilevel procedure we want to estimate the abstract angle between the coarse space and its complementary space in the decomposition of the space at level $(\ell - j)$, $j = 0, 1, \ldots, \ell - 1$; the related element matrices are given by $A_e^{(j)}(\alpha)$, and $A_e^{(j+1)}(\alpha)$, which can be associated with the space at level $(\ell - j)$, and the coarse space at level $(\ell - j)$, respectively.

Unless otherwise specified the parameter α is always assumed to be greater than or equal to one. By construction (cf. (6.2), (6.9)–(6.10)) we have

$$\widehat{A}_{E,22}^{(j)}(\alpha) = A_e^{(j+1)}(\alpha), \tag{6.11}$$

and thus (6.3) can be written as

$$S_E^{(j)}(\alpha) = A_e^{(j+1)}(\alpha) - \widehat{A}_{E,21}^{(j)}(\alpha)(\widehat{A}_{E,11}^{(j)}(\alpha))^{-1}\widehat{A}_{E,12}^{(j)}(\alpha). \tag{6.12}$$

Furthermore, the solution of the local generalized eigenproblem (6.4) is equivalent to finding

$$\begin{aligned} \lambda_{E;\min}^{(2)} &\coloneqq \min_{\mathbf{v} \perp (1,1,\ldots,1)^T} \frac{\mathbf{v}^T S_E^{(j)}(\alpha)\, \mathbf{v}}{\mathbf{v}^T A_e^{(j+1)}(\alpha)\, \mathbf{v}} \\ &= 1 - \max_{\mathbf{v} \perp (1,1,\ldots,1)^T} \frac{\mathbf{v}^T \{\widehat{A}_{E,21}^{(j)}(\alpha)(\widehat{A}_{E,11}^{(j)}(\alpha))^{-1}\widehat{A}_{E,12}^{(j)}(\alpha)\}\, \mathbf{v}}{\mathbf{v}^T A_e^{(j+1)}(\alpha)\, \mathbf{v}}. \end{aligned} \tag{6.13}$$

Now, since it is sufficient to compute a lower bound λ for (6.13) we consider the inequality

$$(1-\lambda)A_e^{(j+1)}(\alpha) - R_E^{(j)}(\alpha) \geqslant 0 \tag{6.14}$$

where

$$R_E^{(j)}(\alpha) = \widehat{A}_{E,21}^{(j)}(\alpha)(\widehat{A}_{E,11}^{(j)}(\alpha))^{-1}\widehat{A}_{E,12}^{(j)}(\alpha). \tag{6.15}$$

Then (6.14) has to be fulfilled with a preferably large $\lambda > 0$. In this regard we first observe the monotonicity of $R_E^{(j)}(\alpha)$ and $A_e^{(j+1)}(\alpha)$.

LEMMA 6.2. *For the transformation Variant 2, the matrix-valued function* $R_E^{(j)} : \alpha \mapsto R_E^{(j)}(\alpha)$, *defined by (6.15), is monotonically decreasing, i.e.* $R_E^{(j)}(\alpha') - R_E^{(j)}(\alpha) \geqslant 0$ *if* $1 \leqslant \alpha' \leqslant \alpha < \infty$. *Furthermore, for fixed* $\alpha \geqslant 1$ *the function* $R_E(\alpha) : j \mapsto R_E^{(j)}(\alpha)$ *decreases in* j, *i.e.,* $R_E^{(j)}(\alpha) - R_E^{(j+1)}(\alpha) \geqslant 0$ *if* $j \in \{1, 2, \ldots\}$. *By contrast, the matrix* $A_e^{(j+1)}(\alpha)$ *is monotonically increasing in* α *and* j.

Proof. From Lemma 6.1 we know that $X_e(\alpha)$ is monotonically increasing and since Y_e is SPSD (and does not depend on α) we conclude that $A_e^{(j)}(\alpha)$ is monotonically increasing in both parameters, α and j.

Then it can be easily checked that for $\alpha \geqslant 1$ the macro-element pivot matrix $\widehat{A}_{E,11}^{(j)}(\alpha)$ is SPD. Thus we have $(\widehat{A}_{E,11}^{(j)}(\alpha))^{-1} \geqslant 0$ showing that $R_E^{(j)}(\alpha) \geqslant 0$. Moreover, since $\widehat{A}_{E,12}^{(j)}(\alpha) = \widehat{A}_{E,12}$ and $\widehat{A}_{E,21}^{(j)}(\alpha) = \widehat{A}_{E,12}^T$ are invariant with respect to α and j, it suffices to show that $\widehat{A}_{E,11}^{(j)}(\alpha)$ is monotonically increasing in both parameters. The latter, however, follows from the fact that $\widehat{A}_{E,11}^{(j)}(\alpha)$ is a special linear combination of three symmetric matrices $A'_{E,11}$, $\bar{A}_{E,11}$ and $\bar{\bar{A}}_{E,11}$, i.e.,

$$\widehat{A}_{E,11}^{(j)}(\alpha) = A'_{E,11} + j\bar{A}_{E,11} + \alpha\bar{\bar{A}}_{E,11}$$

in which $\bar{A}_{E,11}$ and $\bar{\bar{A}}_{E,11}$ are additionally positive semidefinite. Note that neither $\bar{A}_{E,11}$ nor $\bar{\bar{A}}_{E,11}$ depend on α or j! ∎

We are now ready to estimate the angle(s) between the subspaces associated with the multilevel block factorization based on the two-level transformation Variant 2:

THEOREM 6.3. *Consider the elliptic problem (2.1) with constant coefficients discretized by the IP-DG method using bilinear elements on a uniform mesh. The multilevel block factorization in the hierarchical basis (implicitly) generated by recursive application of the two-level transformation, Variant 2 yields a recursive splitting of the related DG-FE spaces for which the following condition holds:*

Considering the splitting at level $\ell - j$, $j \in \{0, 1, \ldots, \ell - 1\}$, *(associated with the* $(j+1)$*-th coarsening step), and assuming that* $\alpha \geqslant \bar{\alpha} \geqslant 1$, *the constant* γ *in the CBS inequality can be estimated locally according to (6.5). In particular, if* $\alpha \geqslant \bar{\alpha} = 4$ *then the local estimate*

$$\gamma \leqslant \gamma_E^{(2)} \leqslant \begin{cases} \sqrt{1 - \left(\frac{9}{14}\right)^2} \approx \sqrt{0.586735} & \text{for } j = 0 \\ \sqrt{1 - \left(\frac{5}{7}\right)^2} \approx \sqrt{0.489796} & \text{for } j > 0 \end{cases} \tag{6.16}$$

holds.

Proof. The proof is based on the inequality (6.14).

Let us first consider the case $j > 0$. We note that the maximum $\lambda > 0$ satisfying inequality (6.14) is given by (6.13). Next, using the assumption $\alpha \geqslant \bar{\alpha} \geqslant 1$ and taking into account the monotonicity properties established by Lemma 6.2 we get

$$(1-\lambda)A_e^{(j+1)}(\alpha) - R_E^{(j)}(\alpha) \geqslant (1-\lambda)A_e^{(2)}(\bar{\alpha}) - R_E^{(1)}(\bar{\alpha}) \quad \forall \lambda > 0,$$

and thus it follows that any $\bar{\lambda} > 0$ satisfying the inequality

$$(1-\bar{\lambda})A_e^{(2)}(\bar{\alpha}) - R_E^{(1)}(\bar{\alpha}) \geqslant 0$$

yields a lower bound for the desired minimum eigenvalue $\lambda_{E;\min}^{(2)}$, i.e.,

$$0 < \bar{\lambda} \leqslant \lambda_{E;\min}^{(2)}.$$

In particular, by choosing $\bar{\alpha} = 4$ (and $j = 1$), and solving the corresponding generalized local eigenvalue problem (6.4), this proves the estimate (6.16) for $j > 0$.

In the case $j = 0$ the bound can be verified by using similar monotonicity arguments (here only the monotonicity with respect to α is required), and finally, choosing again $\alpha = \bar{\alpha}(= 4)$. □

REMARK 6.1. *Comparing the bounds (6.16) and (6.7) it becomes obvious that Variant 2 of the basis transformation is preferable with regard to a stabilization of the condition number at low(er) costs. In this case both inequalities in the optimality condition (4.3) can also be met by employing second-order (instead of third-order) Chebyshev polynomials in the (linear) AMLI cycle.*

REMARK 6.2. *When the (discretization) stabilization parameter α tends to infinity both upper bounds for γ decrease, which shows that the corresponding angles improve. While the limit for Variant 1 of the hierarchical basis is $\sqrt{3/4}$, the limiting value for Variant 2 is given by $\sqrt{3/8}$, which equals the corresponding value for the finite element spaces generated by conforming bilinear elements, i.e.,*

$$\lim_{\alpha \to \infty} \gamma_E^{(2)}(\alpha, j) = \sqrt{3/8} \quad \forall j = 0, 1, 2, \ldots$$

Note that the same limit is obtained for any fixed α as the number of levels tends to infinity, i.e.,

$$\lim_{j \to \infty} \gamma_E^{(2)}(\alpha, j) = \sqrt{3/8} \quad \forall \alpha > 1,$$

which of course is not of practical relevance.

7. Numerical investigations. In this section we present numerical results of two examples which illustrate the theory and demonstrate the potential of our approach.

EXAMPLE 7.1. *Consider the Poisson problem on the unit square $(0,1) \times (0,1)$ with homogenous Dirichlet boundary condition. We choose f such that the analytic solution of the problem is given by $u = x\,(1-x)\,y\,(1-y)\exp(2x+2y)$.*

EXAMPLE 7.2. *Consider the elliptic problem $-\nabla \cdot \underline{A}\nabla u = 1$ on the unit square $(0,1) \times (0,1)$ with homogenous Dirichlet boundary condition. The coefficient $\underline{A}$ has jumps as follows: $\underline{A} = 1$ in $(0, 0.5] \times (0, 0.5] \bigcup (0.5, 1) \times (0.5, 1)$ and $\underline{A} = \varepsilon$ in the remaining domain.*

For all the cases of these examples we use linear polynomial approximations for both the variables x and y. The stabilization parameter α is taken as 5 for the first example and 10 for the second example. The pivot block in the multilevel preconditioner is approximated using the ILU(0) factorization for the first example. However, for the second example with small ε the poor performance of ILU(0) demands a better alternative, and we choose an incomplete factorization based on a drop tolerance (ILU(tol)).[†]

Starting with a random initial guess the following stopping criteria is used

$$\|\mathbf{r}^{(\mathbf{n_{it}})}\|/\|\mathbf{r}^{(\mathbf{0})}\| \leqslant \delta = \mathbf{10^{-6}}.$$

The coarsest mesh in all computations is of size 16×16 and has 1024 DOF. The finer meshes for $1/h = 32, 64, 128, 256, 512$ consist of $4\ 096, \ldots, 1\ 048\ 578$ DOF. For the linear AMLI (LAMLI) W-cycle we used the acceleration polynomial

$$Q^{(k)}(t) \coloneqq \frac{1-P^{(k)}(t)}{t} = \frac{2}{\sqrt{1-\gamma^2}} - \frac{1}{1-\gamma^2}t, \qquad (\gamma^2 \leftarrow 0.5),$$

where the coefficients correspond to the analysis in [6] (for exact inversion of the upper-left pivot block A_{11} in the two-level preconditioner). On the other hand, for the nonlinear AMLI (NLAMLI) W-cycle two inner iterations of generalized conjugate gradient (GCG) type are used at every coarse level except the coarsest (the latter involving a direct solve). The numerical solution of both the examples is plotted in the Figure 7.1.

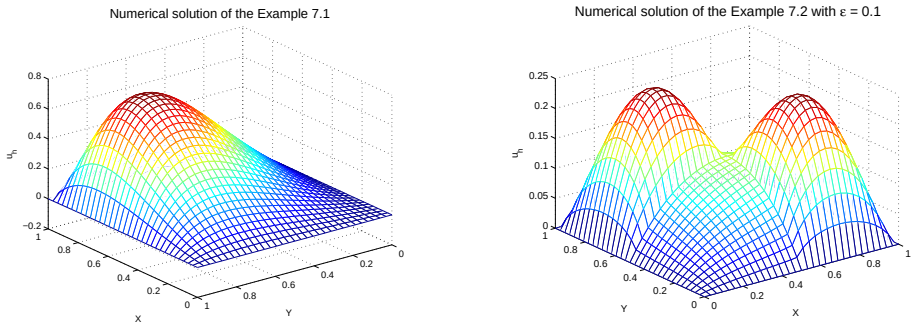

(a) Example 7.1 (b) Example 7.2

FIG. 7.1. *Numerical solution of the examples*

For the example 7.1 we first plot the condition number of the pivot block for $1/h = 256$ against the coarsening steps, see Figure 7.2. This shows the superiority of the Variant 2. However, whereas Variant 1 behaves similarly in both cases (pure Dirichlet or pure Neumann problem), the condition number for the Variant 2 is almost constant for the pure Neumann problem but grows moderately for the pure Dirichlet problem. This growth is attributed to the fact that the face integral term involving the stabilization parameter α in the bilinear form, see (2.3b), is computed only for an internal or a Dirichlet face.

[†]During the computation of the triangular incomplete factors of a matrix M the entries smaller in magnitude than the local drop tolerance (given by the product of the drop tolerance tol and the norm of the corresponding row i of M, i.e. $\text{tol} \cdot \|M_i\|$) are dropped from the appropriate factor [25].

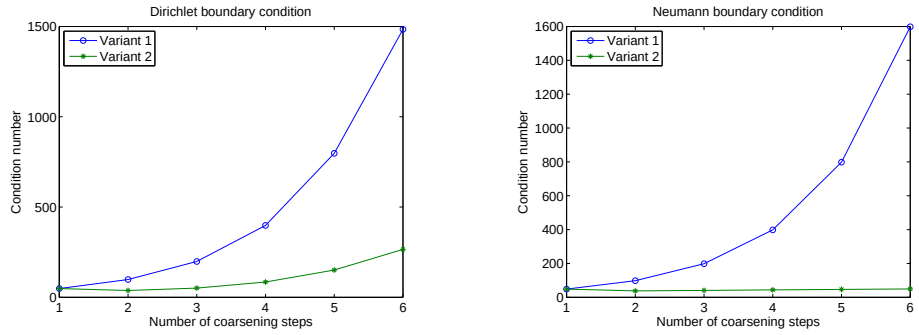

(a) Dirichlet problem (b) Neumann problem

FIG. 7.2. *Condition number of pivot blocks for* $h = 1/256$

TABLE 7.1
Convergence of the AMLI solver for Example 7.1

(a) Linear AMLI (LAMLI) V-cycle

	Variant 1		Variant 2	
$1/h$	n_{it}	ρ	n_{it}	ρ
32	15	0.39	15	0.39
64	23	0.54	20	0.49
128	33	0.66	27	0.60
256	48	0.75	37	0.69
512	67	0.81	49	0.75

(b) AMLI W-cycle for Variant 2

	LAMLI		NLAMLI	
$1/h$	n_{it}	ρ	n_{it}	ρ
32	15	0.39	15	0.39
64	16	0.41	15	0.38
128	16	0.42	15	0.38
256	16	0.42	15	0.38
512	17	0.43	15	0.38

We now discuss the convergence properties of the AMLI solver for Example 7.1. The results for the LAMLI V-cycle for both the variants are presented in the Table 7.1(a). Having illustrated the advantage of the second Variant in Figure 7.2 and Table 7.1(a) we present it's results for AMLI W-cycle for the linear as well as the nonlinear preconditioner in Table 7.1(b). These experiments confirm the theoretical analysis of the previous section.

REMARK 7.1. *It should be noted from Table 7.1(b) that two inner GCG iterations in the variable-step preconditioner (NLAMLI) perform better as compared to the second-degree polynomial stabilization of LAMLI.*

TABLE 7.2
Growth of condition number of the pivot block as ε *gets smaller*

κ	$\varepsilon = 1$	$\varepsilon = 0.1$	$\varepsilon = 0.01$	$\varepsilon = 0.001$
$\kappa(A_{11})$	98.33	997.25	9985.77	99870.73
$\kappa((L_0U_0)^{-1}A_{11})$	28.71	509.01	5609.65	56684.52
$\kappa((L_{\text{tol}}U_{\text{tol}})^{-1}A_{11})$	1.01	1.05	1.13	4.40

Now we discuss the results for Example 7.2. We consider the following cases of the jump coefficient: $\varepsilon = 1, 0.1, 0.01$, and 0.001. Before proceeding further we first present in Table 7.2 the growth of the condition number of the pivot block and preconditioned pivot blocks for the mesh size $1/h = 32$ and varying ε. Two preconditioners

are considered, ILU(0) and ILU(tol), where tol $= 1e-05$. We note that for small values of ε the ILU(0) preconditioner is not efficient and the condition number of the preconditioned system grows with a rate similar to that of A_{11}. Evidently, this lack of robustness is overcome by using ILU(tol), though at approximately 3 times the cost of ILU(0).

TABLE 7.3
Problem 2 ($\varepsilon = 0.001$) - Variants 1 & 2: AMLI V-cycle

	Variant 1		Variant 2	
$1/h$	n_{it}	ρ	n_{it}	ρ
32	12	0.32	12	0.30
64	20	0.49	18	0.46
128	29	0.62	25	0.57
256	42	0.72	34	0.67
512	73	0.83	49	0.76

TABLE 7.4
Problem 2 - Variant 1: NLAMLI W-cycle

	$\varepsilon = 1.0$		$\varepsilon = 0.1$		$\varepsilon = 0.01$		$\varepsilon = 0.001$	
$1/h$	n_{it}	ρ	n_{it}	ρ	n_{it}	ρ	n_{it}	ρ
32	12	0.31	12	0.31	12	0.31	12	0.32
64	13	0.34	13	0.34	13	0.34	14	0.35
128	13	0.34	13	0.34	13	0.34	14	0.36
256	13	0.34	13	0.34	13	0.34	15	0.38
512	13	0.34	13	0.34	13	0.34	15	0.38

TABLE 7.5
Problem 2 - Variant 2: NLAMLI W-cycle

	$\varepsilon = 1.0$		$\varepsilon = 0.1$		$\varepsilon = 0.01$		$\varepsilon = 0.001$	
$1/h$	n_{it}	ρ	n_{it}	ρ	n_{it}	ρ	n_{it}	ρ
32	11	0.28	11	0.28	12	0.29	12	0.30
64	12	0.30	12	0.31	13	0.32	13	0.32
128	11	0.28	12	0.31	12	0.31	12	0.31
256	11	0.28	12	0.30	12	0.31	12	0.31
512	11	0.28	11	0.28	12	0.30	12	0.30

The convergence results of the AMLI solver for V- and W- cycle for Example 7.2 are presented in Tables 7.3–7.5. Even with large jumps in the coefficient (small ε) the results presented in Table 7.3 show a similar convergence behavior as compared to the results for Example 7.1 presented in Table 7.1(a). Now, for varying ε, following the Remark 7.1, we perform an NLAMLI W- cycle. The numerical results are summarized in Tables 7.4–7.5. It can be seen that both variants yield an optimal order method regardless of the variation in the jump in the coefficient. Nevertheless, from Table 7.2 we note that when decreasing ε from 0.01 to 0.001 for a fixed tolerance tol $= 1e-05$ the increase in the condition number of the ILU(tol) preconditioned system is large

as compared to the variation from $\varepsilon = 1.0$ to $\varepsilon = 0.01$. This is related to the decrease in the number of fill-in terms and can be alleviated by taking a smaller tolerance. However, for this fixed tolerance for $\varepsilon = 0.001$ we observe a small deviation from the perfect robustness for Variant 1 in Table 7.4, whereas the results for Variant 2 presented in Table 7.5 show insensitiveness upto this value of ε.

8. Concluding remarks. We presented a framework for constructing and analyzing optimal order two- and multilevel preconditioners for linear systems arising from the symmetric IP-DG discretization of second order elliptic problems. A specific assembling process is proposed where the hierarchy of meshes is geometrically nested. This process is applicable to other similar type of DG discretizations, see Remark 3.1, however, there the analysis of the multilevel preconditioners requires a different focus due to the lack of symmetry and is beyond the scope of this article. The techniques for conforming methods have been extended in such a way that the resulting (algebraic) coarse-grid problems can be associated with a hierarchy of DG discretizations. We considered two different variants of hierarchical splittings and derived the corresponding estimates for the CBS constant related to the angle between the induced subspaces. The obtained bounds show that the overall process for the AMLI W-cycle is of linear complexity, provided that a sufficiently accurate approximation is used for the pivot block A_{11}. Numerical tests on large scale confirm our theoretical investigations. The generalization of the presented approach to three dimensional and anisotropic problems is currently under investigation and is the subject of a separate article.

Acknowledgments. This work was initiated during the Special Radon Semester on Computational Mechanics, held at RICAM, Linz, Oct. 3rd - Dec. 16th 2005, and has been conducted in its follow-up phase. The authors gratefully acknowledge the support by the Austrian Academy of Sciences.

Appendix A. The element matrix A_e.

In this appendix we provide the details of the element matrix A_e. Following (3.7) the matrix A_e is given by

$$A_e = \begin{bmatrix} A_{e;\mathrm{int},\mathrm{int}} & A_{e;\mathrm{int},\mathrm{ext}} \\ A_{e;\mathrm{int},\mathrm{ext}}^T & A_{e;\mathrm{ext},\mathrm{ext}} \end{bmatrix}, \tag{A.1a}$$

where

$$A_{e;\mathrm{int},\mathrm{int}} = \begin{bmatrix} \alpha/3 & \alpha/12 & \alpha/12 & 0 \\ \alpha/12 & \alpha/3 & 0 & \alpha/12 \\ \alpha/12 & 0 & \alpha/3 & \alpha/12 \\ 0 & \alpha/12 & \alpha/12 & \alpha/3 \end{bmatrix}, \tag{A.1b}$$

$$A_{e;\mathrm{int},\mathrm{ext}}^T = \begin{bmatrix} (1-\alpha)/6 & -1/6 & (1-\alpha)/12 & -1/12 \\ (1-\alpha)/12 & -1/12 & (1-\alpha)/6 & -1/6 \\ -1/6 & (1-\alpha)/6 & -1/12 & (1-\alpha)/12 \\ -1/12 & (1-\alpha)/12 & -1/6 & (1-\alpha)/6 \\ (1-\alpha)/6 & (1-\alpha)/12 & -1/6 & -1/12 \\ (1-\alpha)/12 & (1-\alpha)/6 & -1/12 & -1/6 \\ -1/6 & -1/12 & (1-\alpha)/6 & (1-\alpha/12) \\ -1/12 & -1/6 & (1-\alpha)/12 & (1-\alpha)/6 \end{bmatrix}, \tag{A.1c}$$

$$A_{e;\text{ext,ext}} = \begin{bmatrix} \alpha/6 & \alpha/12 & 0 & 0 & 0 & 0 & 0 & 0 \\ \alpha/12 & \alpha/6 & 0 & 0 & 0 & 0 & 0 & 0 \\ 0 & 0 & \alpha/6 & \alpha/12 & 0 & 0 & 0 & 0 \\ 0 & 0 & \alpha/12 & \alpha/6 & 0 & 0 & 0 & 0 \\ 0 & 0 & 0 & 0 & \alpha/6 & \alpha/12 & 0 & 0 \\ 0 & 0 & 0 & 0 & \alpha/12 & \alpha/6 & 0 & 0 \\ 0 & 0 & 0 & 0 & 0 & 0 & \alpha/6 & \alpha/12 \\ 0 & 0 & 0 & 0 & 0 & 0 & \alpha/12 & \alpha/6 \end{bmatrix}. \quad \text{(A.1d)}$$

Here int and ext denote interior and exterior DOF, respectively. For example, in Figure 3.2 the DOF $1, \ldots, 4$ are interior and $5, \ldots, 12$ are exterior.

Now for elements with face(s) $f_s,\ s = 1, \ldots, 4$ lying on $\partial\Omega$ we make the following changes. We have the following correction matrices for respective faces.

$$\widetilde{A}_{e;f_1;\text{int,int}} = \begin{bmatrix} (-2+\alpha)/6 & 1/6 & (-2+\alpha)/12 & 1/12 \\ 1/6 & 0 & 1/12 & 0 \\ (-2+\alpha)/12 & 1/12 & (-2+\alpha)/6 & 1/6 \\ 1/12 & 0 & 1/6 & 0 \end{bmatrix}, \quad \text{(A.2a)}$$

$$\widetilde{A}_{e;f_2;\text{int,int}} = \begin{bmatrix} 0 & 1/6 & 0 & 1/12 \\ 1/6 & (-2+\alpha)/6 & 1/12 & (-2+\alpha)/12 \\ 0 & 1/12 & 0 & 1/6 \\ 1/12 & (-2+\alpha)/12 & 1/6 & (-2+\alpha)/6 \end{bmatrix}, \quad \text{(A.2b)}$$

$$\widetilde{A}_{e;f_3;\text{int,int}} = \begin{bmatrix} (-2+\alpha)/6 & (-2+\alpha)/12 & 1/6 & 1/12 \\ (-2+\alpha)/12 & (-2+\alpha)/6 & 1/12 & 1/6 \\ 1/6 & 1/12 & 0 & 0 \\ 1/12 & 1/6 & 0 & 0 \end{bmatrix}, \quad \text{(A.2c)}$$

$$\widetilde{A}_{e;f_4;\text{int,int}} = \begin{bmatrix} 0 & 0 & 1/6 & 1/12 \\ 0 & 0 & 1/12 & 1/6 \\ 1/6 & 1/12 & (-2+\alpha)/6 & (-2+\alpha)/12 \\ 1/12 & 1/6 & (-2+\alpha)/12 & (-2+\alpha)/6 \end{bmatrix}. \quad \text{(A.2d)}$$

Then for a given face f_s on $\partial\Omega$ the matrix $A_{e;\text{int,int}}$ is modified to $A_{e;\text{int,int}} \pm \widetilde{A}_{e;f_s;\text{int,int}}$, where the sign $\pm$ corresponds to the face being on the Dirichlet boundary or the Neumann boundary, respectively. Furthermore, for the DOF of the neighboring element we make the respective rows and columns of A_e zero.

REFERENCES

[1] D. Arnold, An interior penalty finite element method with discontinuous elements, *SIAM J. Numer. Anal.*, 19 (1982), 742–760.

[2] D. Arnold, F. Brezzi, B. Cockburn, and L. D. Marini, Unified analysis of discontinuous Galerkin methods for elliptic problems, *SIAM J. Numer. Anal.*, 39 (2002), 1749–1779.

[3] O. Axelsson, *Iterative solution methods.* Cambridge University Press, 1994.

[4] O. Axelsson and I. Gustafsson, Preconditioning and two-level multigrid methods of arbitrary degree of approximations, *Math. Comp.*, 40(1983), 219–242.

[5] O. Axelsson and P.S. Vassilevski, Algebraic multilevel preconditioning methods I, *Numer. Math.*, 56 (1989), 157–177.

[6] O. Axelsson and P.S. Vassilevski, Algebraic multilevel preconditioning methods II, *SIAM J. Numer. Anal.*, 27 (1990), 1569–1590.
[7] O. Axelsson and P.S. Vassilevski, Variable-step multilevel preconditioning methods, I: self-adjoint and positive definite elliptic problems, *Num. Lin. Alg. Appl.*, 1 (1994), 75–101.
[8] I. Babuška and M. Zlamal, Nonconforming elements in the finite element method with penalty, SIAM J. Numer. Anal., 10 (1973), 863–875.
[9] R. Bank and T. Dupont, An optimal order process for solving finite element equations, *Math. Comp.*, 36 (1981), 427–458.
[10] C. E. Baumann and J.T. Oden, A discontinuous *hp* finite element method for convection-diffusion problems, *Computer Methods in Applied Mechanics and Engineering*, 175 (1999), 311–341.
[11] R. Blaheta, S. Margenov and M. Neytcheva, Robust optimal multilevel preconditioners for non-conforming finite element systems, *Num. Lin. Alg. Appl.*, 12 (2005), 495–514.
[12] S.C. Brenner and J. Zhao, Convergence of multigrid algorithms for interior penalty methods, *Applied Numerical Analysis and Computational Mathematics*, 2 (2005), 3–18.
[13] F. Brezzi, B. Cockburn, L.D. Marini, and E. Süli. Stabilization mechanisms in discontinuous Galerkin finite element methods. *Report NA-04/24, Oxford University Computing Laboratory*, 2004.
[14] B. Cockburn and C.W. Shu, Runge-Kutta discontinuous Galerkin methods for convection-dominated problems, *Journal of Scientific Computing*, 16(2001), 173–261.
[15] V.A. Dobrev, R.D. Lazarov, P.S. Vassilevski, and L.T. Zikatanov. Two-level preconditioning of discontinuous Galerkin approximations of second order elliptic equations. *Numer. Lin. Alg. Appl.*, 13(2006) 1–18.
[16] J. Douglas Jr., and T. Dupont, *Interior penalty procedures for elliptic and parabolic Galerkin methods, Lecture notes in Phys. 58* Springer-Verlag, Berlin, 1976.
[17] V. Eijkhout and P.S. Vassilevski, The Role of the Strengthened Cauchy-Bunyakowski-Schwarz Inequality in Multilevel Methods, *SIAM Review*, 33(1991), 405–419.
[18] I. Georgiev, J. Kraus, S. Margenov, Multilevel preconditioning of rotated bilinear non-conforming FEM problems, *RICAM-Report 2006-03*, RICAM, Linz, Austria.
[19] J. Gopalkrishnan and G. Kanschat. A multilevel discontinuous Galerkin method. *Numer. Math.*, 95(2003) 527–550.
[20] P.W. Hemker, W. Hoffman, and M.H. van Raalte, Two-level Fourier analysis of a multigrid approach for discontinuous Galerkin discretization, SIAM J. Sci. Comput., 25 (2003), 1018–1041.
[21] J. Kraus, An algebraic preconditioning method for M-matrices: linear versus nonlinear multilevel iteration, *Num. Lin. Alg. Appl.*, 9 (2002), 599–618.
[22] R. Lazarov, S. Margenov, CBS constants for graph-Laplacians and application to multilevel methods for discontinuous Galerkin systems, *RICAM-Report 2005-28*, RICAM, Linz, Austria.
[23] R. Lazarov, P. Vassilevski, L. Zikatanov, Multilevel preconditioning of second order elliptic discontinuous Galerkin problems, Preprint, 2005.
[24] B. Riviere, M.F. Wheeler, and V. Girault, Improved energy estimates for interior penalty, constrained and discontinuous Galerkin methods for elliptic problems I, *Comput. Geosci.*, 3 (1999), 337–360.
[25] Y. Saad, *Iterative Methods for Sparse Linear Systems*, PWS Publishing Company, Boston, 1996.
[26] Ch. Schwab, p- *and* hp- *Finite Element Methods*, Clarendon Press, Oxford, 1998.
[27] K. Shahbazi, An explicit expression for the penalty parameter of the interior penalty method, *Journal of Computational Physics*, 205 (2005), 401–407.
[28] J.J.W. van der Vegt, and S.K. Tomar, Discontinuous Galerkin method for linear free-surface gravity waves, *Journal of Scientific Computing*, 22-23 (2005), 531–567.
[29] M.F. Wheeler, An elliptic collocation-finite element method with interior penalties, SIAM J. Numer. Anal., 15 (1978), 152–161.